Formation of a Semiquinone at the Q_B Site by A- or B-Branch Electron Transfer in the Reaction Center from *Rhodobacter sphaeroides*†

Marion C. Wakeham,‡ Jacques Breton,§ Eliane Nabedryk,§ and Michael R. Jones*,‡

Department of Biochemistry, School of Medical Sciences, University of Bristol, University Walk, Bristol, BS8 1TD, United Kingdom, and Service de Bioénergétique, Bât 532, CEA-Saclay, 91191 Gif-sur-Yvette Cedex, France

Received September 24, 2003; Revised Manuscript Received February 16, 2004

ABSTRACT: In *Rhodobacter sphaeroides* reaction centers containing the mutation Ala M260 to Trp (AM260W), transmembrane electron transfer along the A-branch of cofactors is prevented by the loss of the Q_A ubiquinone. Reaction centers that contain this AM260W mutation are proposed to photoaccumulate the $P^+Q_B^-$ radical pair following transmembrane electron transfer along the B-branch of cofactors (Wakeham, M. C., Goodwin, M. G., McKibbin, C., and Jones, M. R. (2003) Photoaccumulation of the $P^+Q_B^-$ radical pair state in purple bacterial reaction centers that lack the Q_A ubiquinone. *FEBS Lett. 540*, 234−240). The yield of the $P^+Q_B^-$ state appears to depend upon which additional mutations are present. In the present paper, Fourier transform infrared (FTIR) difference spectroscopy was used to demonstrate that photooxidation of the reaction center's primary donor in Q_A-deficient reaction centers results in formation of a semiquinone at the Q_B site by B-branch electron transfer. Reduction of Q_B by the B-branch pathway still occurs at 100 K, with a yield of approximately 10% relative to that at room temperature, in contrast to the Q_A^- to Q_B reaction in the wild-type reaction center, which is not active at cryogenic temperatures. These FTIR results suggest that the conformational changes that "gate" the Q_A^- to Q_B reaction do not necessarily have the same influence on Q_B reduction when the electron donor is the H_B anion, at least in a minority of reaction centers.

In the reaction centers of purple bacteria such as *Rhodobacter* (*Rb.*)[1] *sphaeroides*, light energy is used to drive a membrane-spanning electron-transfer reaction. This triggers a cycle of electron flow that is coupled to the generation of an electrochemical gradient of protons across the bacterial cytoplasmic membrane. The *Rb. sphaeroides* reaction center has been used as a model system for investigating the mechanism of solar energy conversion in photosynthesis (*1*), because it is particularly amenable to spectroscopic analysis (*2*) and X-ray crystal structures are available for the complex (*3*−*9*).

The *Rb. sphaeroides* reaction center is composed of three polypeptides, termed H, L, and M, that bind four bacteriochlorophylls (BChl), two bacteriopheophytins (BPhe), two ubiquinones, a single photoprotective carotenoid, and a nonheme iron atom (Figure 1A). The L- and M-polypeptides form a heterodimeric protein scaffold that arranges the BChl, BPhe, and ubiquinone cofactors in two membrane-spanning branches around an axis of 2-fold symmetry (see Figure 1A and ref *3*−*7*). In the initial steps of energy transduction, light energy drives a transmembrane electron transfer along the so-called A-branch of cofactors from the primary electron donor (P), a pair of excitonically coupled BChl molecules located near the periplasmic side of the membrane, to a molecule of tightly bound ubiquinone (Q_A) located near the cytoplasmic side of the membrane (*2*, *10*−*14*). This transmembrane electron transfer involves an intervening monomeric BChl (B_A) and a molecule of BPhe (H_A) and takes place on a picosecond time scale (*2*, *10*−*14*). The electron residing on the Q_A ubiquinone is passed to the Q_B cofactor binding site, where a loosely bound ubiquinone is reduced to the ubisemiquinone (*15*, *16*). A second light-driven transmembrane electron transfer results in double reduction and double protonation of the Q_B ubisemiquinone to form ubiquinol (*15*, *16*).

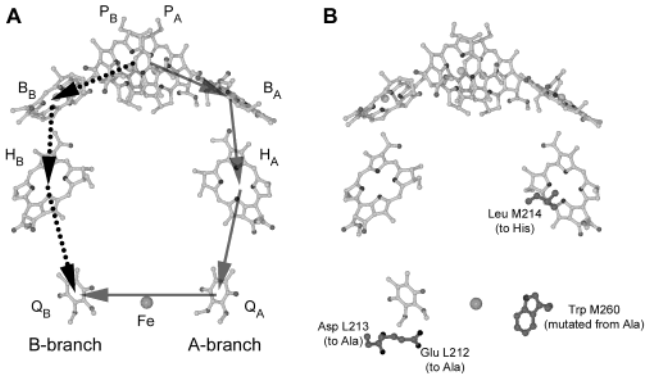

FIGURE 1: Structural models showing (A) cofactor organization in the wild-type reaction center and (B) the AM260W reaction center with the other residues mutated in this paper highlighted. In A, the route of A- and B-branch electron transfer is indicated by the solid and dotted arrows, respectively.

† This work was supported by the Biotechnology and Biological Sciences Research Council of the United Kingdom, the University of Bristol, and the Royal Society.

* To whom correspondence should be addressed: Telephone: (117) 928-7571. Fax: (117) 928-8274. E-mail: m.r.jones@bristol.ac.uk.

‡ University of Bristol.

§ CEA-Saclay.

[1] Abbreviations: B, accessory bacteriochlorophyll; BChl, bacteriochlorophyll; BPhe or H, bacteriopheophytin; FTIR, Fourier transform infrared; P, primary donor of electrons; Q, ubiquinone; *Rb.*, *Rhodobacter*.

10.1021/bi035726x CCC: $27.50
Published on Web 04/01/2004

The selective use of the A-branch of cofactors for transmembrane electron transfer is an intriguing aspect of the design of the purple bacterial reaction center and the related photosystem II reaction center found in oxygenic photosynthetic organisms (*1*). The structural and energetic basis of this asymmetry has been the subject of intense interest, and in recent years mutagenesis has been used in attempts to affect the balance of transmembrane electron transfer along the two branches (*17*−*31*). To date, all of these investigations have involved transient absorption studies in the visible or near infrared, carried out in the presence or absence of inhibitors of ubiquinone reduction at the Q_B site.

In a recent report (*31*), it was shown that a long-lived radical-pair state involving the photo-oxidized primary donor (P^+) could be photoaccumulated in *Rb. sphaeroides* reaction centers that are known to lack the Q_A ubiquinone through mutagenesis of residue alanine M260 to tryptophan (AM260W) (see Figure 1B and ref *32*, *33*). The observed lifetime of this state (seconds) and the fact that its formation was inhibited by the Q_B inhibitor stigmatellin, suggested that this long-lived radical-pair state was $P^+Q_B^-$, formed by electron transfer along the so-called inactive branch (B-branch) of reaction center cofactors (*31*). The yield of this state was increased by combining mutation of Leu M214 to His (LM214H) and a double mutation in which residues Glu L212 and Asp L213 were both changed to Ala (EL212A/DL213A) (see Figure 1B and ref *31*). The former mutation causes a BChl (termed β_A) to be incorporated into the reaction center in place of the native H_A (*17*). The LM214H single mutant reaction center has a slowed rate of A-branch primary forward electron transfer to a state that has a mixed $P^+B_A^-/P^+\beta_A^-$ character (*18*) and shows a decreased yield of electron transfer to the Q_A ubiquinone because of an increased competing decay of the mixed $P^+B_A^-/P^+\beta_A^-$ state to the ground state (*18*). The double alanine substitution makes the reaction center less asymmetric at the level of the quinone binding pockets by making the Q_B binding pocket less polar and so more like the relatively nonpolar Q_A binding pocket (where the symmetry-related residues are Ala M248 and Ala M249) (*34*−*36*). In the wild-type reaction center, Glu L212 and Asp L213 are involved in electron-coupled proton transfer to the Q_B semiquinone (reviewed in *15*, *16*). Replacement of these acidic residues with Ala prevents the transfer of the first proton and second electron to the Q_B semiquinone, producing a very stable $P^+Q_B^-$ state with a lifetime that is 10-fold longer than that in the wild-type complex (*34*). The largest yield of the photoaccumulated $P^+Q_B^-$ state was obtained in a quadruple mutant, denoted WAAH, in which the AM260W, LM214H, and EL212A/DL213A mutations were combined (*31*). The positions of these residues are shown in Figure 1B, which was prepared using the X-ray crystal structure of the AM260W single mutant (*33*).

In the present paper, light-induced Fourier transform infrared (FTIR) difference spectroscopy was used to investigate the nature of the radical-pair state formed by A- or B-branch electron transfer, using infrared marker bands for the P, P^+, Q_A, Q_A^-, Q_B, and Q_B^- states that have been identified in a number of previous studies (*37*−*41*). FTIR difference spectra were recorded for wild-type, WAAH, and EL212A/DL213A (denoted AA) mutant reaction centers, together with a new mutant (denoted WH) in which the AM260W and LM214H mutations are combined. We find that the $P^+Q_B^-$ state is indeed formed by B-branch electron transfer in the WAAH or WH reaction center, and the FTIR difference spectrum of this state is compared with that formed by A-branch electron transfer in the wild-type or AA double mutant reaction center, respectively. The findings are discussed with respect to the different roles of the Q_A and Q_B sites in type II reaction centers.

Table 1: Nomenclature of Mutant Reaction Centers[a]

	amino acid			
name	M260	L212	L213	M214
wild type	Ala	Glu	Asp	Leu
WH	**Trp**	Glu	Asp	**His**
WAAH	**Trp**	**Ala**	**Ala**	**His**
AA	Ala	**Ala**	**Ala**	Leu

[a] Mutations are shown in bold.

EXPERIMENTAL PROCEDURES

Preparation of Experimental Material. The *Rb. sphaeroides* mutant reaction centers used in this paper had the nomenclature described in Table 1. The procedures used in the construction of the WAAH mutant were described recently (*31*). Reaction centers with the double EL212A/DL213A mutation (denoted AA) or the combination AM260W/LM214H (denoted WH) were generated using a similar procedure, which is based on the QuikChange mutagenesis kit (Stratagene). Reaction center *pufLM* genes containing these mutations were expressed in the *Rb. sphaeroides* deletion strain DD13 (*42*), using a derivative of expression vector pRKEH10D that lacks the *pufBA* genes that encode the core LH1 antenna complex (*42*). This produced transconjugant strains that had mutant reaction centers but lacked both types of the light-harvesting complex.

For the preparation of reaction centers, intracytoplasmic membrane fragments were prepared from cells that had been grown under semiaerobic conditions in the dark, using procedures described previously (*43*). Reaction centers were solubilized from membrane fragments suspended in 20 mM Tris/HCl (pH 8.0) by the addition of NaCl to a final concentration of 100 mM followed by LDAO to a final concentration of 1.5%. Solubilized reaction centers were purified by two sequential passes through a DE52 anion exchange column, as described in detail elsewhere (*44*). Purification did not have any significant effects on the visible absorbance spectrum of any of the reaction centers studied (data not shown).

FTIR Spectroscopy. Steady-state light-induced $P^+Q_B^-/PQ_B$ and $P^+Q_A^-/PQ_A$ FTIR difference spectra were recorded either at 285 or 100 K using a Nicolet 860 FTIR spectrometer equipped with a MCT-A detector, a KBr beam-splitter, and a cryostat. Illumination was achieved under saturating actinic light using an RG715 cutoff filter and a water filter to prevent heating of the sample. Each sample of wild-type or mutant reaction centers was reconstituted under argon with 10-fold excess of ubiquinone-3 (Q_3), as described previously (*39*). The reaction center samples were covered with 100 mM Tris-HCl (pH 7) and sealed between two CaF_2 windows, yielding a reaction center concentration of 0.2−0.5 mM. Where appropriate, electron transfer to Q_B was inhibited by 1 mM stigmatellin. The infrared absorbance at the peak of the amide

I band (~1655 cm^{-1}) was kept below 0.8 absorbance units. Cycles of illumination were repeated several hundred times, with a delay between cycles to allow near-to-complete relaxation of light-induced charge-separated states that were adjusted in each experiment to account for the effects of mutations, temperature, and inhibitors on the rate of $P^+Q_A^-$ recombination. In all experiments, the characteristics of the FTIR spectrum did not change over the course of the experiment, demonstrating that there was no detectable degradation of the sample.

RESULTS

Mutant Construction. Reaction centers with the double EL212A/DL213A mutation and the combination AM260W and LM214H were constructed as described in the Experimental Procedures. In agreement with previous studies (*35*), the visible absorbance spectrum of the AA double mutant reaction center was identical to that of the wild-type complex (data not shown). Similarly, the visible absorbance spectrum of the WH mutant reaction center (data not shown) was identical to that previously described for the WAAH mutant complex (*31*). Transient absorbance measurements carried out as described recently (*31*) indicated the photoaccumulation of a P^+-containing state in the WH reaction center that was stable on a millisecond time scale and was sensitive to the Q_B site inhibitor stigmatellin (data not shown). As discussed recently (*31*), the long-lived nature of this state, the absence of the Q_A ubiquinone because of the AM260W mutation, and the inhibitory effect of stigmatellin suggest that this state is $P^+Q_B^-$, formed by electron transfer along the B-branch of cofactors. The activity of the B-branch in the WH reaction center indicated by this measurement was similar to that previously reported for the WAAH reaction center (*31*). A detailed characterization of the WH mutant reaction center will be presented elsewhere.

To compare the final charge separated states produced by A- and B-branch electron transfer in the reaction center, FTIR spectroscopy was first carried out under experimental conditions known to give rise to either a $P^+Q_A^-/PQ_A$ or $P^+Q_B^-/PQ_B$ difference spectrum in the wild-type reaction center (*37*). The $P^+Q_A^-/PQ_A$ and $P^+Q_B^-/PQ_B$ difference spectra in the wild-type reaction center are dominated by contributions from P^+/P, and infrared marker bands for the P, P^+, Q_A, Q_A^-, Q_B, and Q_B^- states have been previously identified (*37*−*41*, *45*).

Evidence for the Lack of a Functional Q_A in Reaction Centers Bearing the AM260W Mutation. Quinone contributions in $P^+Q_A^-/PQ_A$ and $P^+Q_B^-/PQ_B$ spectra have been established through the use of reaction centers reconstituted with isotopically labelled quinones (*38*, *41*). Although Q_A and Q_B are identical molecules (ubiquinone-10, Q_{10}) in native *Rb. sphaeroides* reaction centers, experimentally distinguishable vibrational infrared signatures are observed for Q_A and Q_B in their respective binding sites. For ubiquinone in the Q_A site, a large asymmetry between the two carbonyl groups is observed at 1660 and 1601 cm^{-1}, with a C═C/C═O mode at 1628 cm^{-1} (*39*). For ubiquinone in the Q_B site, the two carbonyl groups contribute equally at 1641 cm^{-1}, while the C═C ring vibrations appear at ~1617 cm^{-1} (*40*). Finally, contribution of the protein to the charge-separated $P^+Q_B^-/PQ_B$ and $P^+Q_A^-/PQ_A$ states is also expected in the amide I (1690−1630 cm^{-1}) and amide II (1560−1530 cm^{-1}) regions. For example, a negative band at 1650 cm^{-1} has been identified in $P^+Q_A^-/PQ_A$ spectra of *Rb. sphaeroides* reaction centers (*37*), while a positive signal is observed in this region in $P^+Q_B^-/PQ_B$ spectra (*37*, *38*).

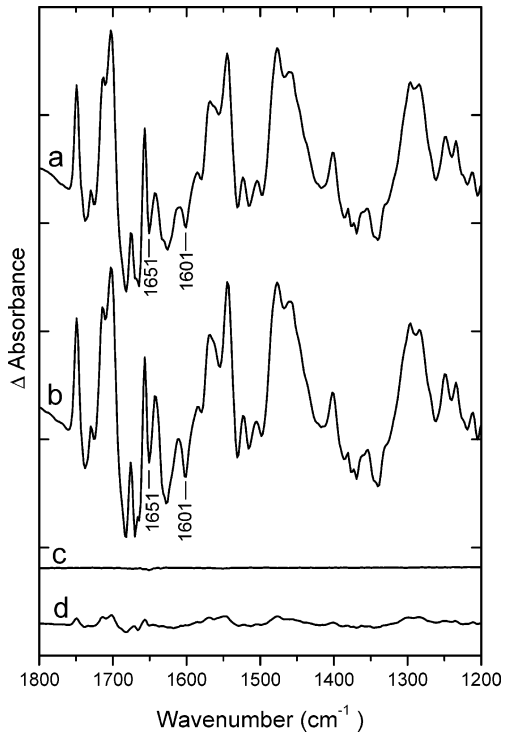

FIGURE 2: Light-induced P^+Q^-/PQ FTIR difference spectra at 285 K of the purified reaction centers in the presence of 1 mM stigmatellin. (a) Wild-type, (b) AA mutant, (c) WH mutant, and (d) WAAH mutant. Spectral resolution was 4 cm^{-1}. A total of 32 000 interferograms were averaged. The tick marks on the vertical axis are separated by 10^{-3} absorbance units.

In the wild-type reaction center, semiquinone formation at the Q_B site is inhibited by stigmatellin, a competitive inhibitor of quinone binding at the Q_B site. In the presence of stigmatellin, the light-induced FTIR difference spectrum obtained at 285 K is characteristic of $P^+Q_A^-/PQ_A$ (Figure 2a), with a negative band at 1601 cm^{-1} that is attributable to the C_4═O carbonyl of the Q_A ubiquinone (*39*) and a negative band at 1651 cm^{-1} that has been attributed to the peptide C═O vibration(s) (*37*). The large positive bands at approximately 1750, 1704, 1550, 1480, and 1295 cm^{-1} arise from P^+ modes (*37*, *38*, *45*).

Before examining the product of electron transfer in the absence of the Q_A ubiquinone in the WAAH and WH reaction centers, we first characterized the effect of the double AA mutation on the light-induced P^+Q^- state formed by conventional A-branch electron transfer. At 285 K, in the presence of stigmatellin, the wild-type and AA mutant reaction centers yielded identical difference spectra (parts a and b of Figure 2, respectively) identified as $P^+Q_A^-/PQ_A$, with negative bands at 1601 and 1651 cm^{-1}. In contrast, the WH reaction center (Figure 2c) gave no difference spectrum in the presence of stigmatellin, and the WAAH reaction center (Figure 2d) gave a spectrum of extremely low amplitude. We believe that the latter was due to a subpopulation of reaction centers that were not inhibited by stigmatellin and in which the $P^+Q_B^-$ state was photoaccumulated. In support of this, we have found that it is not possible to

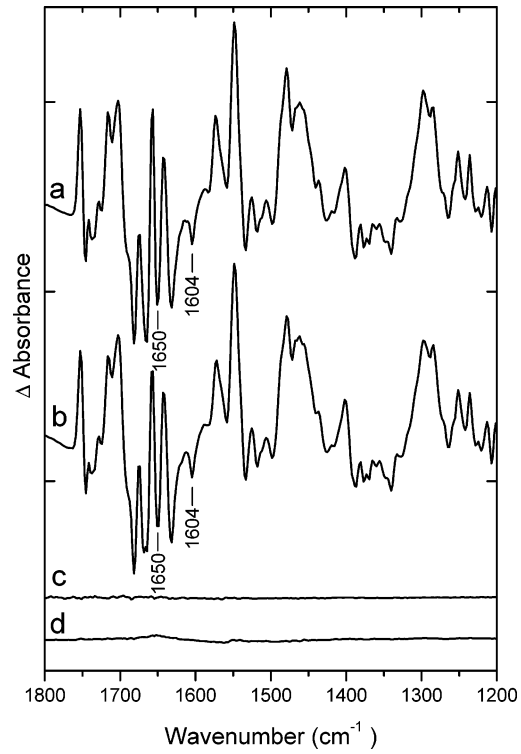

FIGURE 3: Light-induced P^+Q^-/PQ FTIR difference spectra at 100 K of the purified reaction centers in the presence of 1 mM stigmatellin. (a) Wild-type, (b) AA mutant, (c) WH mutant, and (d) WAAH mutant. The experimental parameters were described in the caption to Figure 2. The tick marks on the vertical axis are separated by 10^{-3} absorbance units.

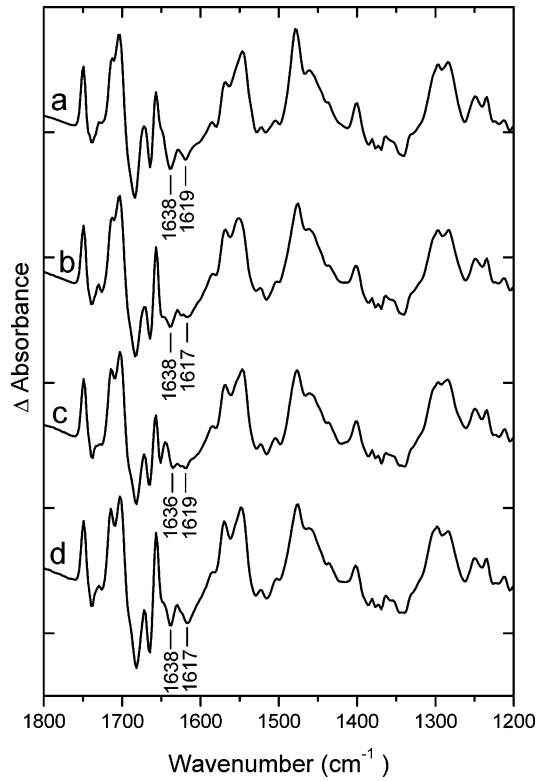

FIGURE 4: Light-induced $P^+Q_B^-$/PQ_B FTIR difference spectra at 285 K of the purified reaction centers reconstituted with excess Q_3. (a) Wild-type, (b) AA mutant, (c) WH mutant, and (d) WAAH mutant. The tick marks on the vertical axis are separated by 3×10^{-3} absorbance units. For comparison, spectra b and c are shown on a 1.5-fold expanded scale, and spectrum d is shown on a 3-fold expanded scale.

fully inhibit $P^+Q_B^-$ formation with stigmatellin in WAAH reaction centers in transient absorbance measurements [(*31*), MCW and MRJ, unpublished observations]. Possibly the combination of the AM260W and AA mutations changes the affinity of the Q_B site for stigmatellin, which would account for the different spectra obtained for the WH and WAAH reaction centers in Figure 2. In support of this, an X-ray crystal structure has been reported for the *Rhodopseudomonas viridis* reaction center with stigmatellin bound at the Q_B site, and this shows that the side chains of both Glu L212 and Asp L213 make close molecular contacts (<4.0 Å) with the stigmatellin headgroup (*46*).

At 100 K, electron transfer from Q_A^- to Q_B is blocked in wild-type reaction centers that have been cooled in the dark (*47*). As a result of this blockage, photoexcitation of wild-type reaction centers at 100 K produces a $P^+Q_A^-$/PQ_A difference spectrum. Such a spectrum is also obtained in the presence of stigmatellin (Figure 3a). At 100 K, the AA mutant reaction centers also produced a $P^+Q_A^-$/PQ_A difference spectrum in the presence of stigmatellin (Figure 3b), as shown by the typical negative bands observed at 1650 and 1604 cm^{-1}. In contrast, the WH and WAAH reaction centers (parts c and d of Figure 3) did not produce a difference spectrum in the presence of this Q_B site inhibitor. For both wild-type and AA reaction centers, a small upshift ($\sim$3 cm^{-1}) of the frequency of the C_4═O carbonyl of Q_A is observed at 100 K compared to 285 K, as previously reported (*39*). These FTIR results demonstrate the absence of a functional Q_A in the WH and WAAH mutant reaction centers, in agreement with the lack of the Q_A ubiquinone in the X-ray crystal structure of the AM260W single mutant (*33*).

Reduction of Q_B by A-Branch Electron Transfer. Parts a and b of Figure 4 compare the FTIR difference spectra obtained at 285 K with wild-type (Figure 4a) and AA (Figure 4b) reaction centers in the absence of stigmatellin. The spectrum obtained with wild-type reaction centers had the characteristics of a $P^+Q_B^-$/PQ_B difference spectrum and was identical to that obtained previously for *Rb. sphaeroides* R-26 reaction centers, with the spectrum being dominated by contributions from P^+/P (*37*, *38*, *45*). The contribution of Q_B^-/Q_B to the spectrum (Figure 4a) was indicated by the negative bands at 1638 and $\sim$1618 cm^{-1} that are characteristic of the C═O and C═C modes of Q_B, respectively.

A similar spectrum was obtained with the AA reaction center (Figure 4b), but the amplitude was approximately two-thirds of that obtained with the wild-type reaction center. This shows that a $P^+Q_B^-$ state is also photoaccumulated in AA mutant reaction centers. In all FTIR difference spectra, the observed amplitude is a function of the concentration of the sample (which was the same between samples to a factor of 2), the relative rates of charge separation and charge recombination, and the delay between the successive light-minus-dark cycles. The amplitudes of the spectra obtained were therefore somewhat variable. However, in all cases, the shape of a particular spectrum was invariant with the amplitude and was dependent only on the radical-pair state that was photoaccumulated. For the purposes of comparison, the data in Figure 4 are shown on different scales (see the figure caption for details).

Another factor that could affect the spectrum obtained with the AA reaction center is a reduction in the occupancy of the Q_B pocket by ubiquinone, caused by the mutation. However, this would be expected to alter the line shape of the spectrum, because light excitation would produce a mixture of $P^+Q_B^-$ and $P^+Q_A^-$ states. Such an alteration was not observed, and so it seems unlikely that the ~30% reduction in signal amplitude can be attributed to a significant reduction in the occupancy of the Q_B site in the AA reaction center, although we cannot rule out the possibility of a small reduction in this occupancy.

Reduction of Q_B by B-Branch Electron Transfer. Figure 4 also shows the spectra obtained at 285 K with the WH (Figure 4c) and WAAH (Figure 4d) reaction centers in the absence of a Q_B site inhibitor. The details of these spectra were similar to those obtained for wild-type and AA reaction centers, providing direct evidence that light excitation leads to the photoaccumulation of the $P^+Q_B^-$ state in the WH and WAAH mutants. Absence of the Q_A ubiquinone is demonstrated by the lack of a negative band for Q_A^- at 1601 cm^{-1} in the spectra displayed in Figure 4. However, the spectrum of the WH reaction center included a small negative peak at 1650 cm^{-1} (Figure 4c). Shoulders were also observed around 1650 cm^{-1} in the spectra of the AA and WAAH reaction centers (parts b and d of Figure 4). This 1650 cm^{-1} signal is not attributed to a Q_A^-/Q_A contribution. Rather, it probably arises from different absorption changes of the protein upon $P^+Q_B^-$ formation in the WH and WAAH reaction centers compared to those in the wild-type complex.

Spectra recorded for reaction centers cooled to 100 K in the dark in the absence of stigmatellin are shown in Figure 5. For the purposes of qualitative comparison, these spectra are also shown on different scales, the details of which are given in the figure caption. The spectra obtained for the wild-type and AA reaction centers (parts a and b of Figure 5) showed features typical of a $P^+Q_A^-/PQ_A$ difference spectrum (*37*), with negative bands at 1604 and 1650 cm^{-1}. In contrast, the difference spectra obtained for the WH and WAAH reaction centers at 100 K (parts c and d of Figure 5) were similar to those obtained at 285 K, showing features typical of a $P^+Q_B^-/PQ_B$ spectrum, with negative bands at ~1635 and 1617 cm^{-1} and no indication of a 1604 cm^{-1} infrared marker band for Q_A. This demonstrates that, while the Q_A^- to Q_B reaction does not occur at 100 K in wild-type reaction centers frozen in the dark (*47*), the reduction of Q_B by B-branch electron transfer and the $P^+Q_B^-$ back reaction are not completely abolished at 100 K in the WH and WAAH reaction centers. However, we note that the yield of $P^+Q_B^-$ was much lower at 100 K than at room temperature, estimated at 10% based on the amplitudes of the protein amide I and II bands in the infrared absorption spectrum of the sample (data not shown).

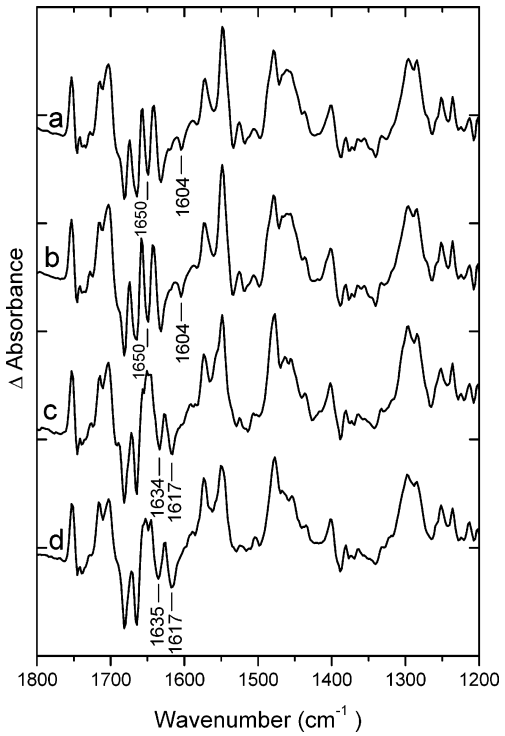

FIGURE 5: Light-induced P^+Q^-/PQ FTIR difference spectra at 100 K of the purified reaction centers reconstituted with excess Q_3. (a) Wild-type, (b) AA mutant, (c) WH mutant, and (d) WAAH mutant. The tick marks on the vertical axis are separated by 2×10^{-3} absorbance units. For the purposes of comparison, the spectra in c and d were measured using a 10-fold greater number of individual scans than those in a and b (this did not affect the characteristics of the spectra) and are shown on a 10-fold expanded scale.

DISCUSSION

To date, investigations of B-branch electron transfer have exclusively involved transient absorption studies in the visible or near infrared, carried out in the presence or absence of inhibitors of ubiquinone reduction at the Q_B site. Most of these studies have concentrated on formation of the $P^+H_B^-$ state (*18*, *20*−*23*, *26*−*28*). Where the possibility of forward electron transfer past $P^+H_B^-$ has been considered, studies have focused on the decay kinetics of the $P^+H_B^-$ state to a presumed $P^+Q_B^-$ state or, as described above, on long-lived (millisecond) absorbance changes associated with P^+ (*19*, *24*, *25*, *29*−*31*). Evidence in support of Q_B reduction via the B-branch has been presented by Laible and co-workers, who reported that the electrochromic changes in BPhe and monomeric BChl absorption that are indicative of the Q_A^- to Q_B reaction were not seen in a mutant *Rb. capsulatus* reaction center that lacks the Q_A ubiquinone but which forms a long-lived P^+Q^- state by B-branch electron transfer (*19*). From infrared vibrational spectroscopy, the present paper provides the first evidence of Q_B reduction via the B-branch of cofactors, making use of infrared marker bands that arise directly from the Q_B ubiquinone (*39*, *40*).

Semiquinone Formation at the Q_B Site as a Result of A- or B-Branch Electron Transfer. Photoexcitation of the WAAH and WH mutant reaction centers at 285 K in the absence of stigmatellin produced an FTIR difference spectrum that was similar to that obtained with AA and wild-type complexes, respectively (Figure 4). The shape of the spectrum suggests that this signal can be attributed to the $P^+Q_B^-$ state, and so the FTIR data provide direct evidence that the $P^+Q_B^-$ radical pair is formed by B-branch electron transfer in the WAAH and WH complexes. The fact that the addition of stigmatellin led to $P^+Q_A^-$ formation in the AA and wild-type reaction centers but abolished P^+Q^- radical-pair formation in the WAAH and WH mutant reaction centers (Figures 2 and 3) confirms that the latter lack a Q_A ubiquinone because of the presence of the AM260W muta-

tion, in line with the interpretation of the data from flash spectroscopy [(*31*), MCW and MRJ, unpublished data].

At 100 K in the absence of stigmatellin, electron transfer from Q_A^- to Q_B in the wild-type and AA reaction centers was abolished, resulting in photoaccumulation of a $P^+Q_A^-$/PQ_A spectrum (parts a and b of Figure 5, respectively). However, it appears that B-branch electron transfer from H_B^- to Q_B was able to proceed in a subpopulation of the WH and WAAH mutant reaction centers (parts c and d of Figure 5, respectively). Therefore, in this fraction of reaction centers, estimated to be approximately 10% of the total, the H_B^- to Q_B reaction is similar to the H_A^- to Q_A reaction that takes place in the wild-type reaction center, in that it is able to proceed at 100 K. The failure of the Q_A^- to Q_B reaction to be operational in wild-type reaction centers cooled in the dark has been taken as evidence that this reaction is conformationally gated or, in other words, that the rate of the reaction is limited by a conformational change that is frozen out at 100 K (*47*). This description of the Q_A^- to Q_B reaction is supported by the observation that the rate of this reaction at room temperature is independent of the driving force for the reaction (*48*), at least for the main ~100 μs component seen in isolated *Rb. sphaeroides* reaction centers (*49*). It would appear that this conformational limitation does not necessarily apply to the reduction of Q_B by H_B^-, because this reaction proceeds in ~10% of the WAAH and WH reaction centers at 100 K, and so one can conclude that whether Q_B reduction is conformationally gated depends on the identity of the electron donor. The 10% most likely corresponds to a subpopulation of reaction centers that are in a permissive conformation for B-branch electron transfer to Q_B at 100 K. The alternative explanation is that this figure of 10% represents the yield of B-branch electron transfer under our excitation conditions; however, given that excitation was achieved using continuous illumination, this seems unlikely. The investigation of the factors that determine this yield is ongoing.

Relevant to this point concerning the activity of the B-branch at cryogenic temperatures, flash-induced absorption changes near 760 nm indicative of $P^+Q_B^-$ formation have been observed at 20 K for a triple GM203D/LM214H/AM260W mutant reaction center from *Rb. sphaeroides*, with 3% of the P-band being bleached by a single, saturating flash. This was interpreted as a 3% yield of $P^+Q_B^-$ formation via the B-branch at 20 K (*25*). In addition, McElroy and coworkers (*50*) have reported a slow ($\tau = 3.5$ s) component in the decay of the P^+Q^- state formed in *Rb. sphaeroides* R-26 reaction centers at 77 K, affecting a "small fraction of the optical and EPR signal". This could be indicative of a minor population of reaction centers that retain the capacity for Q_A^- to Q_B electron transfer at 77 K and so form the relatively long-lived $P^+Q_B^-$ state, or this could indicate a small amount of $P^+Q_B^-$ formation by B-branch electron transfer in reaction centers where the Q_A^- to Q_B is completely frozen out. The latter explanation is interesting in view of the estimated 4% yield of $P^+Q_B^-$ recently reported for the Q_A-deficient AM260W mutant reaction center at room temperature, although the true yield of $P^+Q_B^-$ in this mutant under genuine single-turnover excitation conditions remains to be determined and could be substantially lower than 4% (*31*). The AM260W mutation does not affect the structure of the reaction center outside the Q_A binding site (*32*) or the rate of primary electron transfer from P* to $P^+H_A^-$ (*33*), and so the extent of B-branch electron transfer in the AM260W single mutant could represent the natural activity of the B-branch of cofactors in the wild-type reaction center. In the present experiments on the wild-type or AA mutant at 100 K in the absence of stigmatellin (Figure 5), where a $P^+Q_A^-$ spectrum is obtained because of the freezing out of the Q_A^- to Q_B reaction, the presence of a $P^+Q_B^-$ spectrum arising from a small percentage of the reaction centers would be below the limits of detection. Another point that should be noted is that the conditions of sample illumination during freezing were not given in the report of McElroy and coworkers (*50*), and so it cannot be excluded that the subpopulation of reaction centers giving rise to this signal were locked into the Q_A^- to Q_B permissive conformational state that is obtained with reaction centers that have been frozen under illumination (*47*).

The Binding Position of the Q_B Ubiquinone and Relevance to Conformational Gating. In native reaction centers, the conformational change that gates the Q_A^- to Q_B reaction has been proposed to involve the movement of the Q_B ubiquinone (*48*). Central to this proposal is the observation from X-ray crystallography that the Q_B ubiquinone is capable of occupying two distinct binding positions (*8*, *51*). The first of these, determined for reaction centers frozen to 90 K under illumination, positions the Q_B ubiquinone proximal to the nonheme iron and places the headgroup of the Q_B ubiquinone in a position that is symmetrical with that of the Q_A ubiquinone. The second binding position, determined for reaction centers frozen to 90 K in the dark and described as distal, is located 5 Å closer to the entrance of the Q_B binding pocket. The distal binding conformation has been associated with the oxidized Q_B (dark) state and the proximal conformation with the semiquinone Q_B (light-induced charge-separated) state (*8*). In moving from the distal to proximal position, the headgroup of the Q_B ubiquinone also has to rotate 180° (*8*). This change in binding position of the Q_B ubiquinone has been proposed to be the conformational gate of the Q_A^- to Q_B electron-transfer reaction (*48*), with this movement possibly being triggered by the reduction of Q_A.

Although the model in which electron transfer from Q_A^- to Q_B is gated by the movement of the Q_B ubiquinone is an attractive one, results from X-ray crystallography of mutant complexes (*49*, *52*−*54*) and from FTIR spectroscopy of Q_B reduction in wild-type and mutant reaction centers from *Rb. sphaeroides* (*55*, *56*) have questioned this model. For example, a proximally bound Q_B ubiquinone has been reported in an X-ray crystal structure for a PL209Y mutant reaction center (*53*), on the basis of the diffraction data collected at 5 °C in the dark, but the gating of the Q_A^- to Q_B reaction in this mutant appears to be unaffected because the rate of this reaction is similar to that in the wild-type complex (*57*). A proximally bound Q_B ubiquinone has also been reported in a number of other X-ray crystal structures for mutant reaction centers, including the Q_A-deficient AM260W mutant reaction center (*33*). This last finding questions the proposal that the trigger for the distal-to-proximal movement is the reduction of the Q_A ubiquinone (*33*), although the possible presence of a chloride ion at the vestigial Q_A site in the AM260W reaction center complicates this interpretation (for example, see *58*).

In contrast to the multiple Q_B binding positions found in reaction center X-ray crystal structures, a unique binding site for Q_B has been detected for wild-type (*40*) and several mutant reaction centers (*55*, *56*, *59*) by isotope-edited FTIR difference spectroscopy of Q_B photoreduction. For example, the infrared fingerprint spectra observed for the C═O and C═C modes of Q_B in PL209Y and PL209F mutant reaction centers were similar to that of the wild-type reaction centers, demonstrating that equivalent interactions occur between neutral Q_B and the protein in both wild-type and mutant reaction centers. It was concluded that in all of the reaction centers studied, functional Q_B is locked into a single binding site, which is consistent with the proximal position observed in the X-ray structures, and that the distal/proximal model is not relevant for the gating mechanism that limits the rate of Q_A^- to Q_B electron transfer (*55*, *56*).

The Binding Position of the Q_B Ubiquinone During B-Branch Electron Transfer and the Nature of the $P^+Q_B^-$ State Formed. The present spectroscopic data on WAAH and WH mutants show that the photoreduction of Q_B via B-branch electron transfer occurs at both room temperature and, to a smaller extent, at cryogenic temperature (approximately 10% of that at room temperature). From the discussion above, it is interesting to consider the question of the binding position of the Q_B quinone during B-branch electron transfer. De Boer and co-workers (*25*) have pointed out that the headgroup of the Q_B ubiquinone is closer to H_B when it is in the distal position than when it is in the proximal position, and so electron transfer to a distal Q_B could be favored over transfer to a proximal Q_B in reaction centers where Q_B reduction is achieved via the B-branch. The two binding positions for the Q_B ubiquinone raise the possibility, for example, that the electron transfer from H_B^- to Q_B at 100 K involves only those reaction centers where the Q_B ubiquinone is in the distal position. In the present experiments, there were no significant differences between the $P^+Q_B^-/PQ_B$ FTIR difference spectra established by A- or B-branch electron transfer. From previous FTIR studies (*40*, *55*, *56*, *59*), this suggests that the Q_B ubiquinone is in the proximal site during B-branch electron transfer. However, it should be noted that this spectrum is dominated by contributions from the P^+/P components and gives only limited information on the Q_B^-/Q_B component. Investigations of this issue are ongoing, from FTIR difference spectroscopy with site-specific isotopically labelled ubiquinones.

In a recent report, Laible and co-workers have proposed that the $P^+Q_B^-$ state created by B-branch electron transfer is different from that created by A-branch electron transfer (*29*). The main evidence for this was based on an experiment with a *Rb. capsulatus* reaction center that carries out A- and B-branch electron transfer in parallel. Analysis of the rate of $P^+Q_B^-$ recombination produced the proposal that the $P^+Q_B^-$ radical pair created by B-branch electron transfer recombines directly to the ground state, while the $P^+Q_B^-$ radical pair created by A-branch electron transfer recombines via an indirect route involving a $P^+Q_A^-$ intermediate. In wild-type reaction centers, the latter route plays a dominant role, but the former route is activated in mutant reaction centers in which the free energy of the $P^+Q_B^-$ radical pair is lowered (*60*). One interpretation, therefore, is that the $P^+Q_B^-$ state created by B-branch electron transfer has a lower free energy than that created by A-branch electron transfer (*29*). Another indication of multiple $P^+Q_B^-$ states has been provided by Li and co-workers, who have reported that the fast (<10 μs) phase of the Q_A^- to Q_B reaction seen in *Rb. sphaeroides* membrane-bound reaction centers and complexes with low-potential menaquinones or naphthoquinones reconstituted at Q_A is driving-force-dependent (ref *49* and see the Discussion in ref *61*).

In the present paper, the fact that B-branch electron transfer to Q_B was operational at 100 K in a subfraction of the WH and WAAH reaction centers but A-branch electron transfer was frozen out at this temperature suggests that the conformational change required to achieve Q_B reduction by the A-branch is not necessarily required for Q_B reduction via the B-branch. This difference is interesting, given the proposals of Laible et al. concerning the differences in the product $P^+Q_B^-$ state created by these routes, in terms of its energy and/or protein environment (*29*). From the data presented above, it is apparent that this difference does not affect the FTIR difference spectrum of $P^+Q_B^-$, which was the same regardless of the route of electron transfer from P to Q_B. Clearly, if the nature of any differences between the $P^+Q_B^-$ states formed by A- and B-branch electron transfer could be determined, it could provide valuable insight into the process that gates the Q_A^- to Q_B reaction in wild-type reaction centers.

The Different Roles of Q_A and Q_B in Type II Reaction Centers. To conclude, it seems possible that studies of B-branch electron transfer and exploration of the limitations of this process may finally establish why only one of the two available cofactor branches is used for transmembrane electron transfer in the quinol-producing reaction centers. In the type I reaction centers, where the role of the quinones is to pass single electrons to the iron−sulfur centers, it is becoming apparent that both cofactor branches are used for transmembrane electron transfer (*62*−*64*). In contrast, in all of the type II reaction centers, the A-branch of the cofactors is used to catalyze transmembrane electron transfer, while ubiquinol production is carried out at the Q_B site at the cytoplasmic end of the B-branch, using electrons delivered from the A-branch. This division of responsibility is not seen in the cytochrome bc_1 complexes, where efficient transmembrane electron transfer and ubiquinol production are catalyzed by a single branch of cofactors consisting of two hemes that deliver electrons to a single ubiquinone reductase site. However, in the case of the cytochrome bc_1 complex, this cofactor branch catalyses a cascade of redox reactions that are effectively irreversible, while the cofactor branches in the reaction center face the rather different challenge of very rapidly separating and stabilizing positive and negative charges that have a strong propensity to recombine.

One interesting aspect of research on B-branch electron transfer is that it is providing an opportunity to investigate the practicalities of photoproducing ubiquinol by a single branch of cofactors. These investigations may reveal the limitations that led to the evolution of reaction centers in which the symmetrically located Q_A and Q_B ubiquinones play specialist roles during light-driven ubiquinol production.

ACKNOWLEDGMENT

The authors thank Prof. Peter Rich from the Glynn Laboratory of Bioenergetics, University College London for

helpful discussions and Dr. Paul Fyfe for composing Figure 1.

REFERENCES

1. Heathcote, P., Fyfe, P. K., and Jones, M. R. (2002) Reaction centres: structure and mechanism in biological solar power, *Trends Biochem. Sci. 27*, 79−87.
2. Hoff, A. J., and Deisenhofer, J. (1997) Photophysics of photosynthesis: Structure and spectroscopy of reaction centres of purple bacteria, *Phys. Rep. 287*, 2−247.
3. Allen, J. P., Feher, G., Yeates, T. O., Komiya, H., and Rees, D. C. (1987) Structure of the reaction center from *Rhodobacter sphaeroides* R-26−the cofactors, *Proc. Natl. Acad. Sci. U.S.A. 84*, 5730−5734.
4. Allen, J. P., Feher, G., Yeates, T. O., Komiya, H., and Rees, D. C. (1987) Structure of the reaction center from *Rhodobacter sphaeroides* R-26−the protein subunits, *Proc. Natl. Acad. Sci. U.S.A. 84*, 6162−6166.
5. Chang, C. H., El Kabbani, O., Tiede, D., Norris, J., and Schiffer, M. (1991) Structure of the membrane-bound protein photosynthetic reaction center from *Rhodobacter sphaeroides*, *Biochemistry 30*, 5352−5360.
6. Ermler, U., Fritzsch, G., Buchanan, S. K., and Michel, H. (1994) Structure of the photosynthetic reaction center from *Rhodobacter sphaeroides* at 2.65-angstrom resolution−cofactors and protein-cofactor interactions, *Structure 2*, 925−936.
7. Ermler, U., Michel, H., and Schiffer, M. (1994) Structure and function of the photosynthetic reaction center from *Rhodobacter sphaeroides*, *J. Bioenerg. Biomembr. 26*, 5−15.
8. Stowell, M. H. B., McPhillips, T. M., Rees, D. C., Soltis, S. M., Abresch, E., and Feher, G. (1997) Light-induced structural changes in photosynthetic reaction center: Implications for mechanism of electron-proton transfer, *Science 276*, 812−816.
9. Fyfe, P. K., and Jones, M. R. (2000) Reemerging structures: continuing crystallography of the bacterial reaction centre, *Biochim. Biophys. Acta 1459*, 413−421.
10. Parson, W. W. (1991) Reaction centers, in *Chlorophylls* (Scheer, H., Ed.) pp 1153−1180, CRC Press, Boca Raton, FL.
11. Fleming, G. R., and Van Grondelle, R. (1994) The primary steps of photosynthesis, *Phys. Today 47*, 48−55.
12. Woodbury, N. W., and Allen, J. P. (1995) The pathway, kinetics and thermodynamics of electron transfer in wild type and mutant bacterial reaction centers of purple nonsulfur bacteria, in *Anoxygenic Photosynthetic Bacteria* (Blankenship, R. E., Madigan, M. T., and Bauer, C. E., Eds.) pp 527−557, Kluwer Academic Publishers, Dordrecht, The Netherlands.
13. Parson, W. W. (1996) Photosynthetic bacterial reaction centers, in *Protein Electron Transfer* (Bendall, D. S., Ed.) pp 125−160, BIOS Scientific Publishers, Oxford, U.K.
14. Van Brederode, M. E., and Jones, M. R. (2000) Reaction Centres of Purple Bacteria, in *Enzyme-Catalysed Electron and Radical Transfer* (Scrutton, N. S., and Holzenburg, A., Eds.) pp 621−676, Kluwer Academic/Plenum Publishers, New York.
15. Okamura, M. Y., and Feher, G. (1995) Proton-coupled electron-transfer reactions of Q_B in reaction centers from photosynthetic bacteria, in *Anoxygenic Photosynthetic Bacteria* (Blankenship, R. E., Madigan, M. T., and Bauer, C. E., Eds.) pp 577−594, Kluwer Academic Publishers, Dordrecht, The Netherlands.
16. Okamura, M. Y., Paddock, M. L., Graige, M. S., and Feher, G. (2000) Proton and electron transfer in bacterial reaction centers. *Biochim. Biophys. Acta 1458*, 148−163.
17. Kirmaier, C., Gaul, D., Debey, R., Holten, D., and Schenck, C. C. (1991) Charge separation in a reaction center incorporating bacteriochlorophyll for photoactive bacteriopheophytin, *Science 251*, 922−927.
18. Heller, B. A., Holten, D., and Kirmaier, C. (1995) Control of electron-transfer between the L-side and M-side of photosynthetic reaction centers, *Science 269*, 940−945.
19. Laible, P. D., Kirmaier, C., Holten, D., Tiede, D. M., Schiffer, M., and Hanson, D. K. (1998) Formation of $P^+Q_B^-$ via B-branch electron transfer in mutant reaction centres, in *Photosynthesis: Mechanisms and Effects* (Garab, G., Ed.) pp 849−852, Kluwer, Dordrecht, The Netherlands.
20. Katilius, E., Turanchik, T., Lin, S., Taguchi, A. K. W., and Woodbury, N. W. (1999) B-side electron transfer in a *Rhodobacter sphaeroides* reaction center mutant in which the B-side monomer bacteriochlorophyll is replaced with bacteriopheophytin, *J. Phys. Chem. B. 103*, 7386−7389.
21. Kirmaier, C., Weems, D., and Holten, D. (1999) M-side electron transfer in reaction center mutants with a lysine near the nonphotoactive B bacteriochlorophyll, *Biochemistry 38*, 11516−11530.
22. Kirmaier, C., He, C. Y., and Holten, D. (2001) Manipulating the direction of electron transfer in the bacterial reaction center by swapping Phe for Tyr near BChl(M) (L181) and Tyr for Phe near BChl(L) (M208), *Biochemistry 40*, 12132−12139.
23. Roberts, J. A., Holten, D., and Kirmaier, C. (2001) Primary events in photosynthetic reaction centers with multiple mutations near the photoactive electron carriers, *J. Phys. Chem. B 105*, 5575−5584.
24. de Boer, A. L., Neerken, S., de Wijn, R., Permentier, H. P., Gast, P., Vijgenboom, E., and Hoff, A. J. (2002) High yield of B-branch electron transfer in a quadruple reaction center mutant of the photosynthetic bacterium *Rhodobacter sphaeroides*, *Biochemistry 41*, 3081−3088.
25. de Boer, A. L., Neerken, S., de Wijn, R., Permentier, H. P., Gast, P., Vijgenboom, E., and Hoff, A. J. (2002) B-branch electron transfer in reaction centers of *Rhodobacter sphaeroides* assessed with site-directed mutagenesis, *Photosynth. Res. 71*, 221−239.
26. Kirmaier, C., Laible, P. D., Czarnecki, K., Hata, A. N., Hanson, D. K., Bocian, D. F., and Holten, D. (2002) Comparison of M-side electron transfer in *Rb. sphaeroides* and *Rb. capsulatus* reaction centers, *J. Phys Chem. B 106*, 1799−1808.
27. Katilius, E., Katiliene, Z., Lin, S., Taguchi, A. K. W., and Woodbury, N. W. (2002) B side electron transfer in a *Rhodobacter sphaeroides* reaction center mutant in which the B side monomer bacteriochlorophyll is replaced with bacteriopheophytin: Low-temperature study and energetics of charge-separated states, *J. Phys Chem. B 106*, 1471−1475.
28. Kirmaier, C., Cua, A., He, C. Y., Holten, D., and Bocian, D. F. (2002) Probing M-branch electron transfer and cofactor environment in the bacterial photosynthetic reaction center by addition of a hydrogen bond to the M-side bacteriopheophytin, *J. Phys. Chem. B 106*, 495−503.
29. Laible, P. D., Kirmaier, C., Udawatte, C. S. M., Hofman, S. J., Holten, D., and Hanson, D. K. (2003) Quinone reduction via secondary B-branch electron transfer in mutant bacterial reaction centers, *Biochemistry 42*, 1718−1730.
30. Kirmaier, C., Laible, P. D., Hanson, D. K., and Holten, D. (2003) B-side charge separation in bacterial photosynthetic reaction centers: Nanosecond time scale electron transfer from H_B^- to Q_B, *Biochemistry 42*, 2016−2024.
31. Wakeham, M. C., Goodwin, M. G., McKibbin, C., and Jones, M. R. (2003) Photoaccumulation of the $P^+Q_B^-$ radical pair state in purple bacterial reaction centres that lack the Q_A ubiquinone, *FEBS Lett. 540*, 234−240.
32. Ridge, J. P., van Brederode, M. E., Goodwin, M. G., van Grondelle, R., and Jones, M. R. (1999) Mutations that modify or exclude binding of the Q_A ubiquinone and carotenoid in the reaction center from *Rhodobacter sphaeroides*, *Photosynth. Res. 59*, 9−26.
33. McAuley, K. E., Fyfe, P. K., Ridge, J. P., Cogdell, R. J., Isaacs, N. W., and Jones, M. R. (2000) Ubiquinone binding, ubiquinone exclusion, and detailed cofactor conformation in a mutant bacterial reaction center, *Biochemistry 39*, 15032−15043.
34. Hanson, D. K., Baciou, L., Tiede, D. M., Nance, S. L., Schiffer, M., and Sebban, P. (1992) In bacterial reaction centers protons can diffuse to the secondary quinone by alternative pathways, *Biochim. Biophys. Acta 1102*, 260−265.
35. Hanson, D. K., Tiede, D. M., Nance, S. L., Chang, C.-H., and Schiffer, M. (1993) Site-specific and compensatory mutations imply unexpected pathways for proton delivery to the Q_B binding-site of the photosynthetic reaction-center, *Proc. Natl. Acad. Sci. U.S.A. 90*, 8929−8933.
36. Maróti, P, Hanson, D. K., Baciou, L., Schiffer, M., and Sebban, P. (1994) Proton conduction within the reaction centers of *Rhodobacter capsulatus*−the electrostatic role of the protein, *Proc. Natl. Acad. Sci. U.S.A. 91*, 5617−5621.
37. Nabedryk, E., Bagley, K. A., Thibodeau, D. L., Bauscher, M., Mäntele, W., and Breton, J. (1990) A protein conformational change associated with the photoreduction of the primary and secondary quinones in the bacterial reaction center, *FEBS Lett. 266*, 59−62.
38. Bagley, K., Abresch, E., Okamura, M. Y., Feher, G., Bauscher, M., Mäntele, W., Nabedryk, E., and Breton, J. (1990) FTIR studies

of the $D^+Q_A^-$ and $D^+Q_B^-$ states in reaction centers from *Rb. sphaeroides*, in *Current Research in Photosynthesis* (Baltscheffsky, M., Ed.) pp 75−85, Springer, Berlin, Germany.
39. Breton, J., Boullais, C., Burie, J.-R., Nabedryk, E., and Mioskowski, C. (1994) Binding-sites of quinones in photosynthetic bacterial reaction centers investigated by light-induced FTIR difference spectroscopy—assignment of the interactions of each carbonyl of Q_A in *Rhodobacter sphaeroides* using site-specific C-13-labeled ubiquinone, *Biochemistry 33*, 14378−14386.
40. Breton, J., Boullais, C., Berger, G., Mioskowski, C., and Nabedryk, E. (1995) Binding-sites of quinones in photosynthetic bacterial reaction centers investigated by light-induced FTIR difference spectroscopy—symmetry of the carbonyl interactions and close equivalence of the Q_B vibrations in *Rhodobacter sphaeroides* and *Rhodopseudomonas viridis* probed by isotope labeling, *Biochemistry 34*, 11606−11616.
41. Breton, J., and Nabedryk, E. (1996) Protein-quinone interactions in the bacterial photosynthetic reaction center: Light-induced FTIR difference spectroscopy of the quinone vibrations, *Biochim. Biophys. Acta 1275*, 84−90.
42. Jones, M. R., Fowler, G. J. S., Gibson, L. C. D., Grief, G. G., Olsen, J. D., Crielaard, W., and Hunter, C. N. (1992) Construction of mutants of *Rhodobacter sphaeroides* lacking one or more pigment-protein complexes and complementation with reaction-centre, LH1, and LH2 genes, *Mol. Microbiol. 6*, 1173−1184.
43. Jones, M. R., Heer-Dawson, M., Mattioli, T. A., Hunter, C. N., and Robert, B. (1994) Site-specific mutagenesis of the reaction centre from *Rhodobacter sphaeroides* studied by Fourier transform Raman spectroscopy: Mutations at tyrosine M210 do not affect the electronic structure of the primary donor, *FEBS Lett. 339*, 18−24.
44. McAuley-Hecht, K. E., Fyfe, P. K., Ridge, J. P., Prince, S. M., Hunter, C. N., Isaacs, N. W., Cogdell, R. J., and Jones, M. R. (1998) Structural studies of wild type and mutant reaction centres from an antenna-deficient strain of *Rhodobacter sphaeroides*: monitoring the optical properties of the complex from cell to crystal, *Biochemistry 37*, 4740−4750.
45. Nabedryk, E. (1996) Light-induced Fourier transform infrared difference spectroscopy of the primary electron donor in photosynthetic reaction centers, in *Infrared Spectroscopy of Biomolecules* (Mantsch, H. H., and Chapman, D., Eds.) pp 39−81, Wiley-Liss, New York.
46. Lancaster, C. R., and Michel, H. (1997) The coupling of light-induced electron transfer and proton uptake as derived from crystal structures of reaction centres from *Rhodopseudomonas viridis* modified at the binding site of the secondary quinone, Q_B, *Structure 5*, 1339−1359.
47. Kleinfeld, D., Feher, G., and Okamura, M. Y. (1984) Electron-transfer kinetics in photosynthetic reaction centers cooled to cryogenic temperatures in the charge-separated state—evidence for light-induced structural-changes, *Biochemistry 23*, 5780−5786.
48. Graige, M. S., Feher, G., and Okamura, M. Y. (1998) Conformational gating of the electron-transfer reaction $Q_A^-Q_B \rightarrow Q_AQ_B^-$ in bacterial reaction centers of *Rhodobacter sphaeroides* determined by a driving force assay, *Proc. Natl. Acad. Sci. U.S.A. 95*, 11679−11684.
49. Li, J., Takahashi, E., and Gunner, M. R. (2000) $-\Delta G°_{AB}$ and pH dependence of electron transfer from $P^+Q_A^-Q_B$ to $P^+Q_AQ_B^-$ in *Rhodobacter sphaeroides* reaction centers, *Biochemistry 39*, 7445−7454.
50. McElroy, J. D., Feher, G., and Mauzerall, D. C. (1969) On the nature of the free radical formed during the primary process of bacterial photosynthesis, *Biochim. Biophys. Acta 172*, 180−183.
51. Fritzsch, G., Koepke, J., Diem, R., Kuglstatter, A., and Baciou, L. (2002) Charge separation induces conformational changes in the photosynthetic reaction centre of purple bacteria, *Acta Crystallogr., Sect. D 58*, 1660−1663.
52. Pokkuluri, P. R., Laible, P. D., Deng, Y.-L., Wong, T. N., Hanson, D. K., and Schiffer, M. (2002) The structure of a mutant photosynthetic reaction center shows unexpected changes in main chain orientations and quinone position, *Biochemistry 41*, 5998−6007.
53. Kuglstatter, A., Ermler, U., Michel, H., Baciou, L., and Fritzsch, G. (2001) X-ray structure analyses of photosynthetic reaction center variants from *Rhodobacter sphaeroides*: Structural changes induced by point mutations at position L209 modulate electron and proton transfer, *Biochemistry 40*, 4253−4260.
54. Spiedel, D., Roszak, A. W., McKendrick, K., McAuley, K. E., Fyfe, P. K., Nabedryk, E., Breton, J., Robert, B., Cogdell, R. J., Isaacs, N. W., and Jones, M. R. (2002) Tuning of the optical and electrochemical properties of the primary donor bacteriochlorophylls in the reaction center from *Rhodobacter sphaeroides*: spectroscopy and structure, *Biochim. Biophys. Acta*, *1554*, 75−93.
55. Breton, J., Boullais, C., Mioskowski, C., Sebban, P., Baciou, L., and Nabedryk, E. (2002) Vibrational spectroscopy favors a unique Q_B binding site at the proximal position in wild-type reaction centers and in the Pro-L209 → Tyr mutant from *Rhodobacter sphaeroides*, *Biochemistry 41*, 12921−12927.
56. Nabedryk, E., Breton, J., Sebban, P., and Baciou, L. (2003) Quinone (Q_B) binding site and protein structural changes in photosynthetic reaction center mutants at Pro-L209 revealed by vibrational spectroscopy, *Biochemistry 42*, 5819−5827.
57. Xu, Q., Baciou, L., Sebban, P., and Gunner, M. R. (2002) Exploring the energy landscape for Q_A^- to Q_B electron transfer in bacterial photosynthetic reaction centers: Effect of substrate position and tail length on the conformational gating step, *Biochemistry 41*, 10021−10025.
58. Zachariae, U., and Lancaster, C. R. D. (2001) Proton uptake associated with the reduction of the primary quinone Q_A influences the binding site of the secondary quinone Q_B in *Rhodospeudomonas viridis* photosynthetic reaction centers, *Biochim. Biophys. Acta 1505*, 280−290.
59. Breton, J., Nabedryk, E., Boullais, C., Mioskowski, C., Paddock, M. L., Feher, G., and Okamura, M. Y. (1997) Interaction of Q_B and Q_B^- with the protein in native and Ser-223 → Ala *Rb. sphaeroides* reaction centers probed by light-induced FTIR difference spectroscopy, *Biophys. J. 72*, A7.
60. Takahashi, E., and Wraight, C. A. (1992) Proton and electron-transfer in the acceptor quinone complex of *Rhodobacter sphaeroides* reaction centers—characterization of site-directed mutants of the 2 ionizable residues, GluL212 and AspL213, in the Q_B binding-site, *Biochemistry 31*, 855−866.
61. Xu, Q., and Gunner, M. R. (2001) Trapping conformational intermediate states in the reaction center protein from photosynthetic bacteria, *Biochemistry*, *40*, 3232−3241.
62. Joliot, P., and Joliot, A. (1999) In vivo analysis of the electron transfer within Photosystem-I: are the two phylloquinones involved? *Biochemistry 38*, 11130−11136.
63. Guergova-Kuras, M., Boudreaux, B., Joliot, A., Joliot, P., and Redding, K. (2001) Evidence for two active branches for electron transfer in Photosystem-I, *Proc. Natl. Acad. Sci U.S.A. 98*, 4437−4442.
64. Purton, S., Stevens, D. R., Muhiuddin, I. P., Evans, M. C. W., Carter, S., Rigby, S. E. J., and Heathcote, P. (2001) Site-directed mutagenesis of PsaA residue W693 affects phylloquinone binding and function in the Photosystem I reaction center of *Chlamydomonas reinhardtii*, *Biochemistry 40*, 2167−2175.

BI035726X